Article

Synthesis and Characterization of Water Soluble Single-Walled Carbon Nanotube Graft Copolymers

Bin Zhao, Hui Hu, Aiping Yu, Daniel Perea, and Robert C. Haddon

J. Am. Chem. Soc., **2005**, 127 (22), 8197-8203• DOI: 10.1021/ja042924i • Publication Date (Web): 12 May 2005

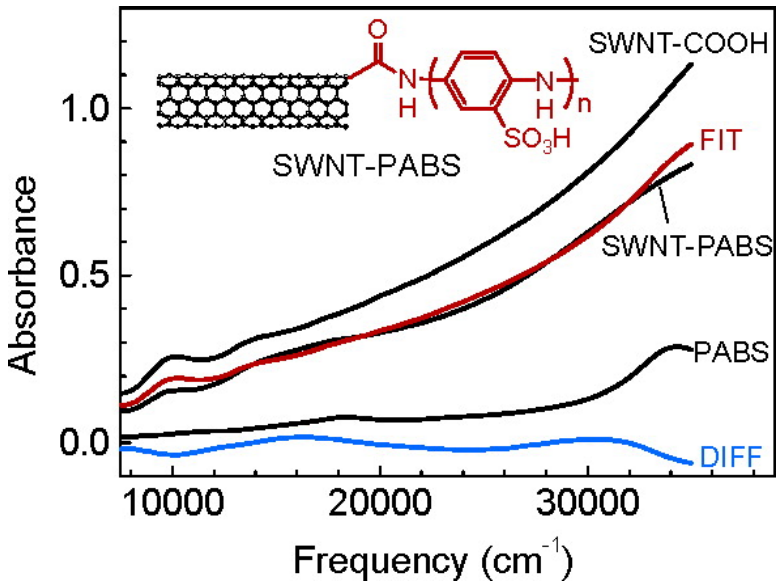

More About This Article

Additional resources and features associated with this article are available within the HTML version:

- Supporting Information
- Links to the 16 articles that cite this article, as of the time of this article download
- Access to high resolution figures
- Links to articles and content related to this article
- Copyright permission to reproduce figures and/or text from this article

View the Full Text HTML

J|A|C|S
ARTICLES
Published on Web 05/12/2005

Synthesis and Characterization of Water Soluble Single-Walled Carbon Nanotube Graft Copolymers

Bin Zhao, Hui Hu, Aiping Yu, Daniel Perea, and Robert C. Haddon*

Contribution from the Center for Nanoscale Science and Engineering Departments of Chemistry and Chemical & Environmental Engineering, University of California, Riverside, California 92521-0403

Received November 23, 2004; E-mail: robert.haddon@ucr.edu

Abstract: Poly(aminobenzene sulfonic acid) (PABS) and polyethylene glycol (PEG) were covalently attached to single-walled carbon nanotubes (SWNTs) to form water-soluble graft copolymers. Quantitative near-IR (NIR) spectroscopic studies of these SWNT graft copolymers indicate a water solubility of about 5 mg/mL, and atomic force microscopy studies show a fairly uniform length and diameter. On the basis of thermogravimetric analysis, the loading of SWNTs in the graft copolymers is estimated to be 30% for SWNT−PABS and 71% for SWNT−PEG. NIR spectroscopic studies of SWNT−PABS show that this graft copolymer has a ground state that is a hybrid of the electronic structures of the isolated PABS and SWNT macromolecules.

Introduction

The synthesis of water-soluble carbon nanotubes is an important topic because such materials have potential applications in biology and materials science. It has been reported that water-soluble carbon nanotubes can be produced by functionalization with polymers,[1−10] crown ethers,[11] glucosamines,[12] biological molecules such as DNA,[13] peptides,[14] proteins,[15] and through sidewall functionalization.[16] Physical wrapping or encapsulation of carbon nanotubes with poly(vinylpyrrolidone) (PVP) and polystyrene sulfonate (PSS),[17] surfactants,[18−21] polystyrene−poly(acrylic acid) copolymer,[22] starch,[23] natural polymer,[24] or by adjusting the pH of the solution[25] can also improve the solubility of carbon nanotubes in water.

Polyaniline (PANI) is a conducting polymer that has received special attention as a result of its high stability toward air and moisture, high electrical conductivity, and unique redox properties. Recently PANI and PANI derivatives have been employed to make composite materials with carbon nanotubes.[26−28] PANI substituted by alkyl-,[29] alkoxy-,[30−33] and alkyl-N-substituted[34] were reported to be soluble in organic solvents. Among these materials, sulfonated PANIs (SPAN)[35−39] are of great interest

(1) Riggs, J. E.; Guo, Z.-X.; Carroll, D. L.; Sun, Y. P. *J. Am. Chem. Soc.* **2000**, *122*, 5879−5880.
(2) Riggs, J. E.; Walker, D. B.; Carroll, D. L.; Sun, Y.-P. *J. Phys. Chem. B* **2000**, *104*, 7071−7076.
(3) Fu, K.; Huang, W.; Lin, Y.; Riddle, L. A.; Carroll, D. L.; Sun, Y.-P. *Nano Lett.* **2001**, *1*, 439−441.
(4) Sun, Y. P.; Huang, W.; Lin, Y.; Kefu, Y.; Kitaygorodskiy, A.; Riddle, L. A.; Yu, Y.; Caroll, D. L. *Chem. Mater.* **2001**, *13*, 2864−2869.
(5) Czerw, R.; Guo, Z.; Ajayan, P. M.; Sun, Y. P.; Carroll, D. L. *Nano Lett.* **2001**, *1*, 423−427.
(6) Sano, M.; Kamino, A.; Okamura, J.; Shinkai, S. *Langmuir* **2001**, *17*, 5125−5128.
(7) Huang, W.; Lin, Y.; Taylor, S.; Gaillard, J.; Rao, A. M.; Sun, Y.-P. *Nano Lett.* **2002**, *2*, 231−234.
(8) Hill, D. E.; Lin, Y.; Rao, A. M.; Allard, L. F.; Sun, Y. P. *Macromolecules* **2002**, *35*, 9466−9471.
(9) Lin, Y.; Rao, A. M.; Sadanadan, B.; Kenik, E. A.; Sun, Y. P. *J. Phys. Chem. B* **2002**, *106*, 1294−1298.
(10) Zhao, B.; Hu, H.; Haddon, R. C. *Adv. Func. Mater.* **2004**, *14*, 71−76.
(11) Kahn, M. G. C.; Banerjee, S.; Wong, S. S. *Nano Lett.* **2002**, *2*, 1215−1218.
(12) Pompeo, F.; Resasco, D. E. *Nano Lett.* **2002**, *2*, 369−373.
(13) Hazani, M.; Naaman, R.; Hennrich, F.; Kappes, M. M. *Nano Lett.* **2003**, *3*, 153−155.
(14) Pantarotto, D.; Partidos, C. D.; Graff, R.; Hoebeke, J.; Briand, J. P.; Prato, M.; Bianco, A. *J. Am. Chem. Soc.* **2003**, *125*, 6160−6164.
(15) Huang, W.; Taylor, S.; Fu, K.; Lin, Y.; Zhang, D.; Hanks, T. W.; Rao, A. M.; Sun, Y.-P. *Nano Lett.* **2002**, *2*, 311−314.
(16) Georgakilas, V.; Kordatos, K.; Prato, M.; Guldi, D. M.; Holzinger, M.; Hirsch, A. *J. Am. Chem. Soc.* **2002**, *124*, 760−761.
(17) O'Connell, M. J.; Boul, P.; Ericson, L. M.; Huffman, C.; Wang, Y.; Haroz, E.; Kuper, C.; Tour, J.; Ausman, K. D.; Smalley, R. E. *Chem. Phys. Lett.* **2001**, *342*, 265−271.
(18) Zhang, X.; Liu, T.; Sreekumar, T. V.; Kumar, S.; Moore, V. C.; Hauge, R. H.; Smalley, R. E. *Nano Lett.* **2003**, *3*, 1285−1288.
(19) Islam, M. F.; Rojas, E.; Bergey, D. M.; Johnson, A. T.; Yodh, A. G. *Nano Lett.* **2003**, *3*, 269−273.
(20) Dyke, C. A.; Tour, J. M. *Nano Lett.* **2003**, *3*, 1215−1218.
(21) Jiang, L.; Gao, L.; Sun, J. *J. Colloid Interface Sci.* **2003**, *260*, 89−94.
(22) Kang, Y.; Taton, T. A. *J. Am. Chem. Soc.* **2003**, *125*, 5650−5651.
(23) Star, A.; Steuerman, D. W.; Heath, J. R.; Stoddart, J. F. *Angew. Chem., Int. Ed* **2002**, *41*, 2508−2512.
(24) Bandyopadhyaya, R.; Nativ-Roth, E.; Regev, O.; Yerushalmi-Rozen, R. *Nano Lett.* **2002**, *2*, 25−28.
(25) Zhao, W.; Song, C.; Pehrsson, P. E. *J. Am. Chem. Soc.* **2002**, *124*, 12418−12419.
(26) Zengin, H.; Zhou, W.; Jin, J.; Czerw, R.; Smith, J. D. W.; Echegoyen, L.; Carroll, D. L.; Foulger, S. H.; Ballato, J. *Adv. Mater.* **2002**, *14*, 1480−1483.
(27) Valter, B.; Ram, M. K.; Nicolini, C. *Langmuir* **2002**, *18*, 1535−1541.
(28) Blanchet, G. B.; Fincher, C. R.; Gao, F. *Appl. Phys. Lett.* **2003**, *82*, 1290−1292.
(29) Wei, Y.; Focke, W. W.; Wnek, G. E. *J. Phys. Chem.* **1989**, *93*, 495−499.
(30) Macinnes, J. D.; Funt, B. L. *Synth. Met.* **1988**, *25*, 235−242.
(31) Dhawan, S. K.; Trivedi, D. C. *Synth. Met.* **1993**, *60*, 67−71.
(32) Storrier, G. D.; Colbran, S. B.; Hibbert, D. B. *Synth. Met.* **1994**, *62*, 179−186.
(33) Feng, W.; Fujii, A.; Lee, S.; Wu, H. C.; Yoshino, K. *Synth. Met.* **2001**, *121*, 1595−1596.
(34) Chen, S.; Huang, G. *J. Am. Chem. Soc.* **1995**, *117*, 10055−10062.
(35) Cao, Y.; Andreatta, A.; Heeger, A. J.; Smith, P. *Polymer* **1989**, *30*, 2305.
(36) Wei, X. L.; Wang, Y. Z.; Long, S. M.; Bobeczko, C.; Epstein, A. J. *J. Am. Chem. Soc.* **1996**, *118*, 2545−2555.
(37) Ito, S.; Murata, K.; Teshima, S.; Aizawa, R.; Asako, Y.; Takahashi, K.; Hoffman, B. M. *Synth. Met.* **1998**, *96*, 161−163.
(38) Roy, B. C.; Dutta Gupta, M.; Bhowmik, L.; Ray, J. K. *Synth. Met.* **1999**, *100*, 233−236.

because of their unique electroactive properties, self-doping, thermal stability, characteristic optical properties, and water solubility. As a result, SPANs have generated interest in the areas of rechargeable batteries,[40,41] light-emitting diode devices,[42] junction devices,[43] and in the electrochemical control of electrolyte acidity and enzyme activity.[44]

Very recently, we reported the synthesis of a water-soluble single-walled carbon nanotube poly(*m*-aminobenzene sulfonic acid) graft copolymer (SWNT−PABS).[10] The SWNTs employed in this work were produced by the HiPco method and are known to possess a relatively small diameter. The SWNT−PABS graft copolymer has excellent water solubility and exhibits an order of magnitude increase in electrical conductivity over neat PABS. This material formulation has found application as the active electronic component in an ammonia sensor,[45] and its zwitterionic electronic structure and water solubility have been exploited in biological studies on the interaction of neurons with carbon nanotubes.[46] As we show below, SWNT−PABS is the first nanotube-based graft copolymer that has a ground state that is a hybrid of the electronic structures of the isolated macromolecular components. In this paper, we report the synthesis of two water-soluble SWNT−graft copolymers by covalent functionalization of SWNTs with PABS and poly(ethylene glycol) (PEG) at gram scale; the starting SWNTs were produced by the electric arc (EA) method and are known to be of larger diameter than HiPco material.[47] The solubility of SWNT−PABS and SWNT−PEG graft copolymers is about 5 mg/mL according to quantitative optical spectroscopy studies. While SWNT−PEG is a simple material in which the electronic structure of the SWNT component is unperturbed by functionalization, we provide evidence that SWNT−PABS is the first covalently functionalized material for which an internally doped electronic structure can be demonstrated. The loading of SWNTs in the graft copolymers has been investigated by thermogravimetric analysis (TGA). The ζ potential of SWNT−PABS has been measured in order to obtain information on the mechanism of dissolution.

Experimental Section

Purified (P3), EA SWNTs were obtained from Carbon Solutions, Inc. (www.carbonsolution.com); to denote the presence of the carboxylic acid functionality, P3−SWNT material is sometimes referred to as SWNT−COOH. The P3−SWNT material is specifically tailored for functionalization chemistry, and it contains 6% carboxylic acid groups[48] and a relative carbonaceous purity of 70−90%.[49] All other chemicals were purchased from Aldrich and used as received. Mid-IR spectra were measured on a Nicolet Magna-IR 560 ESP spectrometer. The solution-phase near-IR (NIR) spectra were measured on a Varian Cary 500 spectrometer. Atomic force microscopy (AFM) images were taken on a Digital Instruments nanoscope IIIA (using taping mode). Scanning electron microscopy (SEM) images were taken on a Philips SEM XL-30 microscope. TGA data were recorded on a Perkin-Elmer Instruments, Pyris Diamond TG/DTA Thermogravimetric/Differential Thermal Analyzer, with a heating rate of 5°C/min in air. ζ potential data were recorded on a Zetaplus Analyzer (Zetaplus, Brookhaven, USA).

SWNT−PABS Graft Copolymer. P3−SWNTs (500 mg) were sonicated in 500 mL of dimethylformamide (DMF) for 2 h to give a homogeneous suspension. Oxalyl chloride (20 mL) was added dropwise to the SWNT suspension at 0 °C under N_2. The mixture was stirred at 0 °C for 2 h and then at room temperature for another 2 h. Finally the temperature was raised to 70 °C, and the mixture was stirred overnight to remove excess oxalyl chloride. PABS[38] (5 g) dissolved in DMF was added to the SWNT suspension, and the mixture was stirred at 100 °C for 5 days. After it was cooled to room temperature, the mixture was filtered through a 0.2-μm pore-size membrane and washed thoroughly with DMF, ethyl alcohol, and deionized (DI) water. The black solid was collected on the membrane and dried under vacuum overnight (1.6 g).

SWNT−PEG Graft Copolymer. P3−SWNTs (1.5 g) were sonicated in 800 mL of DMF for 2 h to give a homogeneous suspension. The SWNT suspension was reacted with oxalyl chloride (60 mL), using the same procedure as was used in the preparation of SWNT−PABS. PEG (15 g, from Aldrich, MW = 600) was added to the SWNT suspension, and the mixture was stirred at 100 °C for 5 days. After it was cooled to room temperature, the mixture was filtered through a 0.2-μm pore-size membrane and washed thoroughly with ethyl alcohol and DI water. The black solid was collected on the membrane and dried under vacuum overnight (1.2 g).

Solubility. A 0.1 mg/mL aqueous solution of the SWNT derivative was prepared by the sonication of 5.0 mg of the material in 50.0 mL of DI water for 2 h. The resulting homogeneous brown solution was diluted with DI water to prepare 0.05, 0.02, and 0.01 mg/mL solutions for NIR characterization, and the NIR spectra of the SWNT derivative solutions were measured immediately after preparation of the solution. A saturated solution of the SWNT derivative was prepared by the sonication of 20 mg of material in 2 mL of DI water for 2 h. The resulting suspension was allowed to stand overnight at room temperature. The upper layer was carefully removed with a syringe and diluted with DI water. The diluted upper layer was used for the NIR spectroscopic estimation of the concentration of material in the saturated aqueous solution, and the solubilities of SWNT−COOH, SWNT−PABS, and SWNT−PEG were determined as 0.7, 5.8, and 5.9 mg/mL, respectively. To check this result on the bulk scale, 50 mg of SWNT−PABS was sonicated in 10 mL of water. The concentration of SWNT−PABS in solution was measured immediately after sonication and again after 2 days standing to give solubility values of 5.2 and 4.8 mg/mL.

Results and Discussion

Synthesis. The synthesis of SWNT−PABS and SWNT−PEG graft copolymers are illustrated in Scheme 1. The starting EA P3−SWNTs were obtained from Carbon Solutions Inc.; this material is terminated with carboxylic acid groups and has a relative carbonaceous purity of 70−90%.[49] The carboxylic acid functionalized material (P3, SWNT−COOH), was reacted with oxalyl chloride to form the acyl chloride intermediate, which was reacted with PABS and PEG to form the corresponding graft copolymers. Dilute solutions of SWNT−PABS and SWNT−PEG in water are gray-black, whereas aqueous solutions of PABS are purple, and aqueous solutions of PEG are colorless. The graft copolymers are quite stable, can be synthesized on the gram scale, and are candidates for industrial

(39) Roy, B. C.; Gupta, M. D.; Bhoumik, L.; Ray, J. K. *Synth. Met.* **2002**, *130*, 27−33.
(40) Barbero, C.; Miras, M. C.; Kotz, R.; Haas, O. *Synth. Met.* **1993**, *55*, 1539−1544.
(41) Barbero, C.; Miras, M. C.; Schnyder, B.; Haas, O.; Kotz, R. *J. Mater. Chem.* **1994**, *4*, 1775−1783.
(42) Ferreira, M.; Rubner, M. F. *Macromolecules* **1995**, *28*, 7107−7114.
(43) Narasimhan, M.; Hagler, M.; Cammarata, V.; Thakur, M. *Appl. Phys. Lett.* **1998**, *72*, 1063−1065.
(44) Yue, J.; Epstein, A. *J. Chem. Soc., Chem. Commun.* **1992**, 1540−1542.
(45) Bekyarova, E.; Davis, M.; Burch, T.; Itkis, M. E.; Zhao, B.; Sunshine, S.; Haddon, R. C. *J. Phys. Chem. B* **2004**, *108*, 19717−19720.
(46) Hu, H.; Ni, Y.; Montana, V.; Haddon, R. C.; Parpura, V. *Nano Lett.* **2004**, *4*, 507−511.
(47) Hamon, M. A.; Itkis, M. E.; Niyogi, S.; Alvaraez, T.; Kuper, C.; Menon, M.; Haddon, R. C. *J. Am. Chem. Soc.* **2001**, *123*, 11292−11293.
(48) Hu, H.; Bhowmik, P.; Zhao, B.; Hamon, M. A.; Itkis, M. E.; Haddon, R. C. *Chem. Phys. Lett.* **2001**, *345*, 25−28.
(49) Itkis, M. E.; Perea, D.; Niyogi, S.; Rickard, S.; Hamon, M.; Hu, H.; Zhao, B.; Haddon, R. C. *Nano Lett.* **2003**, *3*, 309−314.

Scheme 1. Synthesis of SWNT−PABS and SWNT−PEG Graft Copolymers

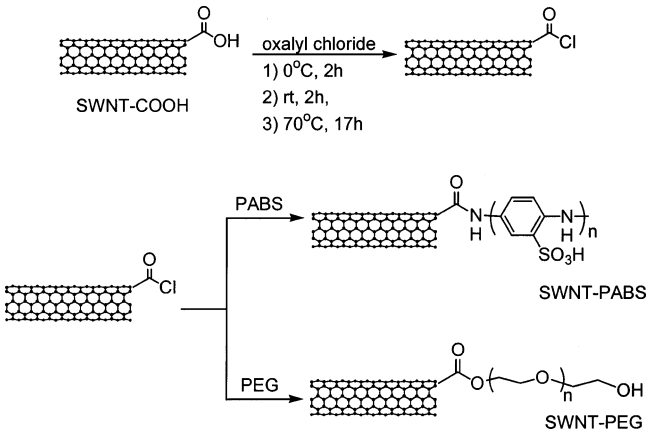

applications, particularly in biological applications requiring water solubility.

Mid-IR spectra (ATR method) of SWNT−COOH, SWNT−PABS, and SWNT−PEG are shown in Figure 1. The peaks due to the carbonyl stretches of these materials show good correspondence to the expected structure of the SWNTs. The spectrum of the starting material (SWNT−COOH) shows a signal at 1705 cm^{-1}, which is due to the carbonyl stretch of the carboxylic acid group.[50,51] The spectra of SWNT−PABS and SWNT−PEG show absorbances at 1649 and 1740 cm^{-1}, which can be assigned to the carbonyl vibration of the amide and ester, respectively.[50,51]

TGA Measurements and SWNT Loading. In our previous work, energy-dispersive X-ray spectroscopy (EDS) was used to study the loading of SWNTs in the SWNT−PABS graft copolymer, and we found that the SWNT component constituted about 17 wt % of the graft copolymer.[10] In the present study, we used TGA to analyze the loading of SWNTs in the graft copolymers, but since the decomposition temperature of PABS (420 °C) is close to the combustion temperature of SWNTs, TGA measurements do not provide a clear separation between the two components. Figure 2 shows the TGA graphs and the derivative curves of SWNT−COOH, SWNT−PABS, and SWNT−PEG. The weight percentage of metal residue is 8.7% for SWNT−COOH, 3.2% for SWNT−PABS, and 6.2% for SWNT−PEG, whereas neat PABS did not leave a residue. We repeated the measurement for SWNT−PABS because NIR spectroscopy cannot be used to check the TGA result (below). On the basis of these measurements, we estimate the loading of SWNTs in SWNT−PABS and SWNT−PEG to be about 30 and 71%, respectively. This result is roughly consistent with the synthetic yield of the products together with the reactivity of the starting materials (320% for SWNT−PABS and 80% for SWNT−PEG, based on the weight of the SWNT−COOH starting material) and is also supported by NIR measurement on SWNT−PEG that give a SWNT loading of 72% (see below). The difference in the loading is probably a result of the low reactivity of PEG toward SWNT−COCl; the amine functionality on PABS is a superior nucleophile to the alcohol on PEG. The loading of SWNTs in the arc SWNT−PABS is higher than that

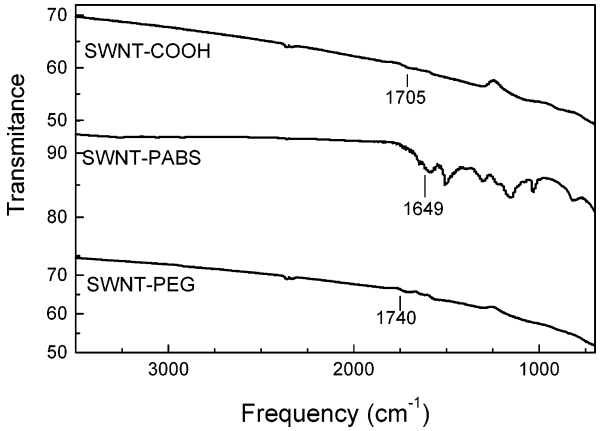

Figure 1. Mid-IR spectra (ATR method) of SWNT−COOH (top), SWNT−PABS (middle), and SWNT−PEG (bottom).

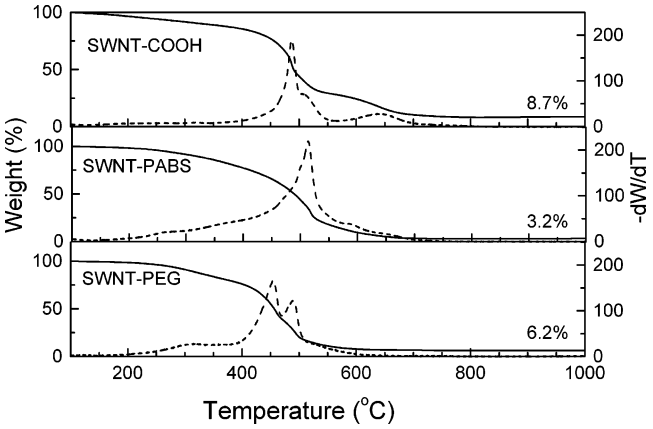

Figure 2. TGA graphs and derivative curves of SWNT samples. The TGA graphs are labeled with the wt % of metal residue after ramping the sample to 1000 °C.

attained in the HiPco SWNT−PABS graft copolymer,[10] which indicates that more PABS was attached to the HiPco SWNTs. The loading of SWNTs in the graft copolymer presumably reflects the concentration of carboxylic acid groups on the SWNTs and the cleavage of the carbon nanotube bundles. The HiPco SWNTs used in our previous work were shortened by HNO_3/H_2SO_4 treatment,[52] and this may be responsible for the higher concentration of carboxylic acid functional groups and the higher degree of SWNT debundling.

By use of the determination of the SWNT loading in the graft copolymers, it is possible to estimate the fraction of the carbon atoms in the SWNTs that become functionalized in the copolymers. For example, the molecular weight of PEG used in the research is about 600, so the degree of functionality in SWNT−PEG can be calculated as a molar functionality = (29/600)/(71/12) = 1%. Thus only about 1% of the carbons in the SWNTs are functionalized with PEG; the same calculation gives a degree of functionality in SWNT−PABS of 4%. The concentration of carboxylic acid groups in the SWNT−COOH starting material was determined to be 6% by acid−base titration,[48] and thus a significant fraction of these residues are retained in the SWNT−PEG and SWNT−PABS graft copolymers.

(50) Chen, J.; Hamon, M. A.; Hu, H.; Chen, Y.; Rao, A. M.; Eklund, P. C.; Haddon, R. C. *Science* **1998**, *282*, 95−98.
(51) Hamon, M. A.; Chen, J.; Hu, H.; Chen, Y.; Itkis, M. E.; Rao, A. M.; Eklund, P. C.; Haddon, R. C. *Adv. Mater.* **1999**, *11*, 834−840.
(52) Liu, J.; Rinzler, A. G.; Dai, H.; Hafner, J. H.; Bradley, R. K.; Boul, P. J.; Lu, A.; Iverson, T.; Shelimov, K.; Huffman, C. B.; Rodriguez-Macias, F.; Shon, Y.-S.; Lee, T. R.; Colbert, D. T.; Smalley, R. E. *Science* **1998**, *280*, 1253−1255.

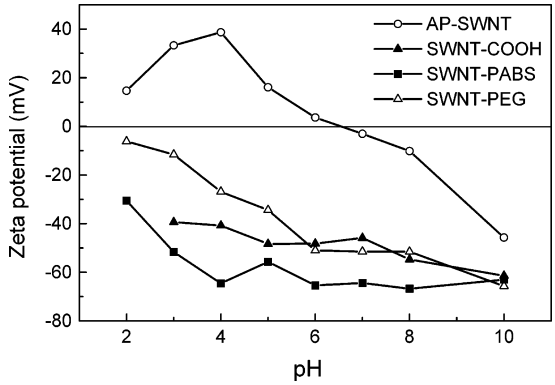

Figure 3. ζ potential of aqueous SWNTs samples at a concentration of 0.05 mg/mL.

ζ Potential Measurements. The ζ potential provides an indicator of the stability of colloidal systems. Measurements of the ζ potential have already been used to discuss the density of acidic sites on the surface of multiwalled carbon nanotubes (MWNTs) and the stability of MWNT/water colloidal systems.[21,53−58] The ζ potential of a series of aqueous SWNT samples as a function of pH is shown in Figure 3; the absolute value of the ζ potential over a wide pH range (2−10) follows the order: SWNT−PABS > SWNT−COOH > SWNT−PEG > as-prepared (AP) SWNTs, which is consistent with the surface charge of these materials. SWNT−PABS contains sulfonic acid and amine groups that exist in zwitterionic form, and thus it has the highest charge throughout the pH range. The absolute value of the ζ potential of SWNT−PABS is larger than 30mV over a wide pH range (from 2 to 10), which indicates that it is very stable in water at a concentration of 0.05 mg/mL. The aqueous dissolution mechanism of the PABS moiety can be attributed to the dominance of the electrostatic and steric repulsion between the functionalized SWNTs over the van der Waals attraction that leads to coagulation and precipitation. SWNT−PEG has less charge than SWNT−COOH since the functionalization converts the carboxylic acid groups into esters, nevertheless the solubility of SWNT−PEG is very close to that of SWNT−PABS presumably due to the oxygen-containing glycol chain which can form hydrogen bonds with the water molecules and capture cations present in solution. The absolute value of the ζ potential of AP SWNTs is less than 30 mV from pH 5 to 8 as expected from the inert graphene surface of the pristine SWNTs, and this indicates that the system has insufficient electrostatic repulsion to maintain its stability at a concentration of 0.05 mg/mL.

Nevertheless, the behavior of the AP SWNT sample supports the idea that electrolytes can preferentially adhere to the carbon nanotube surface.[59] For example, electrophoretic deposition experiments showed that SWNTs migrated toward the positive electrode in the presence of NaOH but toward the negative electrode when $MgCl_2$ was in solution with the carbon nanotubes.[59]

AFM and SEM. AFM images (Figure 4) of the graft copolymers were obtained by drying aqueous solutions on mica substrates. SWNT−COOH has an average length of 890 nm

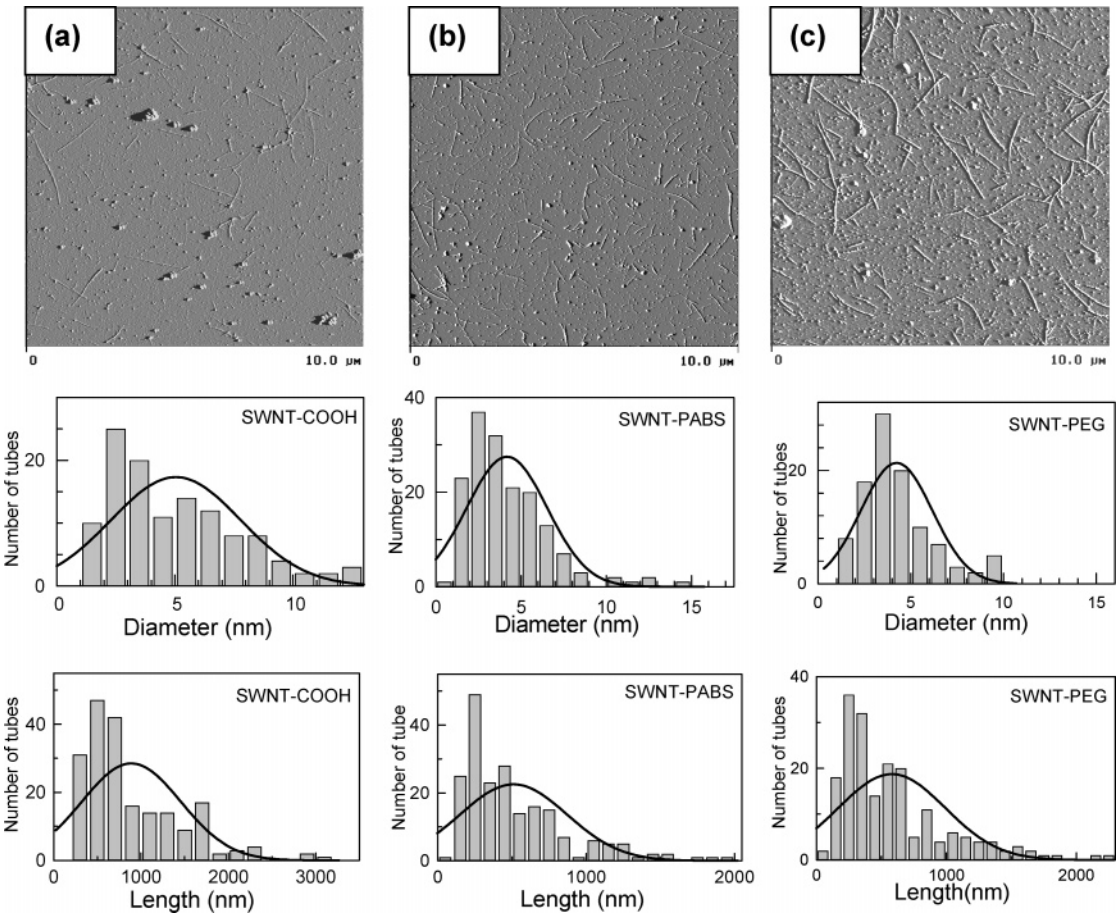

Figure 4. AFM images of (a) SWNT−COOH, (b) SWNT−PABS, and (c) SWNT−PEG. The length and diameter distribution of the graft copolymers are obtained from the AFM images.

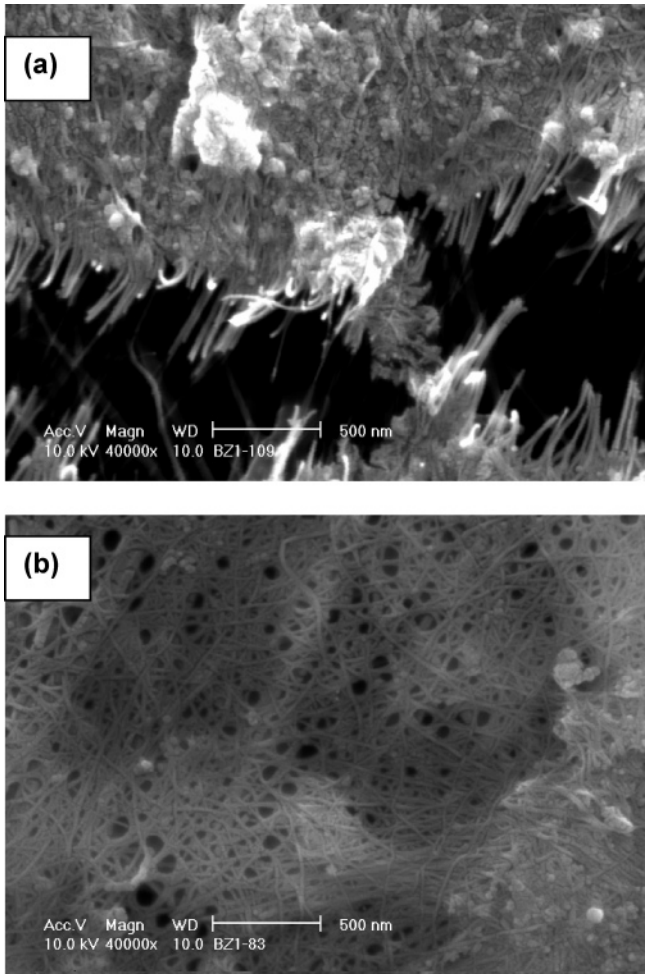

Figure 5. SEM images of (a) SWNT−PABS and (b) SWNT−PEG.

and average diameter of 5.04 nm. The average length of SWNT−PABS is about 510 nm, with an average diameter of 4.2 nm. A large number of the nanotubes (63%) in the SWNT−PABS graft copolymer have a length shorter than 500 nm, and only a small amount of tubes are longer than 1 μm (11%). About 82% of the tubes in SWNT−PABS have bundle sizes less than 6 nm. The average length and diameter of SWNT−PEG is 580 and 4.3 nm, respectively. In fact, the PABS and PEG attached to the surface of SWNTs should increase the effective diameter of the SWNTs. So the exact bundle size of the SWNTs is likely to be smaller than the observed values; it is not uncommon for functionalization reactions to exfoliate the SWNT bundles.

SEM images of SWNT−PABS and SWNT−PEG (Figure 5) show that the SWNTs dominate the morphology of both of the graft copolymers. The SEM image of SWNT−PABS shows that the SWNTs are entrapped in PABS matrix to give a compositelike appearance,[10] while the image of SWNT−PEG shows a dispersed network of interconnected SWNTs.

Electronic Spectroscopy, Solubility, and Electronic Structure. Solution-phase UV spectroscopy has been used to demonstrate a linear relationship between the absorbance and solution concentration of soluble carbon nanotubes in dichlorobenzene,[60] chloroform,[4,9] tetrahydrofuran,[8,61] DMF,[62,63] and water.[15] However, a quantitative solubility study of functionalized SWNTs in water has not been reported, and we have used solution-phase NIR spectroscopy to investigate the solubility of SWNT−PABS and SWNT−PEG in water. A series of

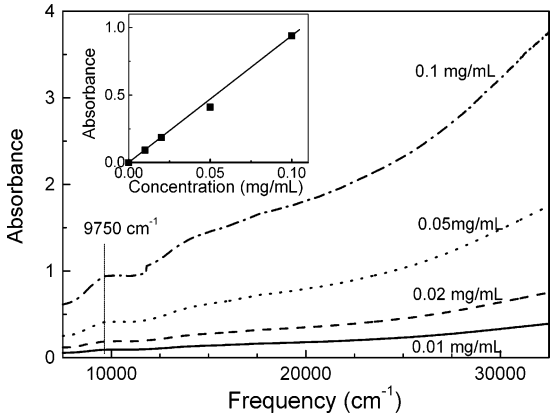

Figure 6. Solution phase NIR spectra of SWNT−PABS in water. The inset is the plot of absorbance versus concentration (mg/mL) for the SWNT−PABS standard solutions. Slope = 9.28, R^2 = 0.997.

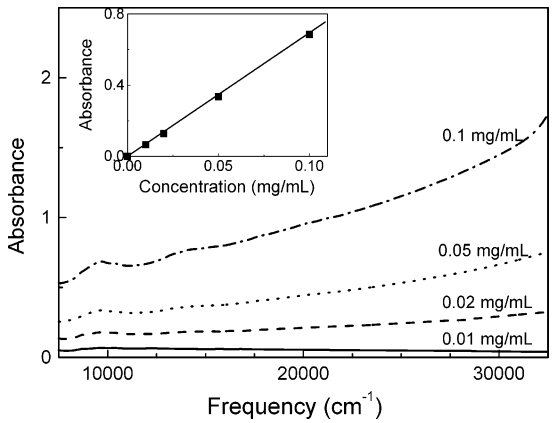

Figure 7. Solution-phase NIR spectra of SWNT−PEG in water. The inset is the plot of absorbance vs concentration (mg/mL) for the SWNT−PEG standard solutions. Slope = 6.87, R^2 = 0.999.

standard solutions (0.1, 0.05, 0.02, and 0.01 mg/mL) were prepared to calibrate the solubility of the graft copolymers by measuring the intensity of the absorption at the second pair of singularities in the density of states (DOS) of the semiconducting SWNTs (S_{22}, centered at 9750 cm^{-1}, Figures 6 and 7). The S_{22} interband transition is characteristic of the SWNTs and has been used to evaluate the purity of electric arc produced SWNTs.[49,62−65] By measurement of the intensity of the S_{22} interband transition (9750 cm^{-1}) of saturated solutions, the solubility of SWNT−PABS and SWNT−PEG are found to be 5.8 and 5.9 mg/mL, respectively. Application of our previous method[62,63] to the results obtained for SWNT−COOH, SWNT−PABS, SWNT−PEG, and PABS gives aqueous effective extinction coefficients of 12.8, 7.3, 9.2, and 1.3 L·g^{-1}·cm^{-1} at 9750 cm^{-1}, respectively. The effective extinction coefficient found for the SWNT−COOH material in water (191 L·mol^{-1}·cm^{-1}) is lower than the values we reported for highly purified samples in DMF.[62,63]

Because PEG is optically transparent throughout the Vis−NIR region and remains electronically inert in the copolymer, it is straightforward to use the above spectral data to calculate the loading of SWNTs in the SWNT−PEG graft copolymer.

(53) Esumi, K.; Ishigami, M.; Nakajima, A.; Sawada, K.; Honda, H. *Carbon* **1996**, *34*, 279−281.
(54) Miller, S. A.; Young, V. Y.; Martin, C. R. *J. Am. Chem. Soc.* **2001**, *123*, 12335−12342.
(55) Sun, J.; Gao, L.; Li, W. *Chem. Mater.* **2002**, *14*, 5169−5172.
(56) Kim, B.; Park, H.; Sigmund, W. M. *Langmuir* **2003**, *19*, 2525−2527.

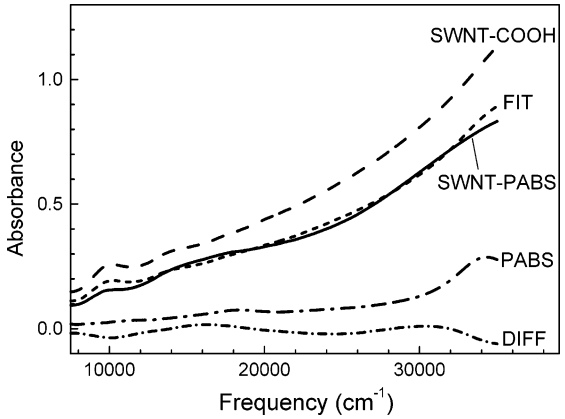

Figure 8. NIR spectra of SWNT−PABS copolymer (solid line), SWNT−COOH (dashed line), PABS (long dash−dotted line) in water at a concentration of 0.02 mg/mL. The short dashed line is a fit of the function FIT = $K(a(\text{PABS}) + b(\text{SWNT−COOH}))$ to the SWNT−PABS spectrum, which gave $K = 1.0$, $a = 0.22$, and $b = 0.78$. The short dash−dotted line is the difference spectrum obtained from the function DIFF = SWNT−PABS − FIT.

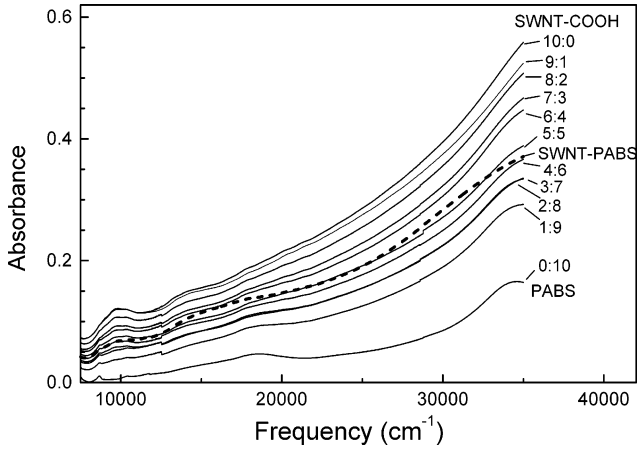

Figure 9. NIR spectra of mixtures of SWNT−COOH and PABS in water at constant total concentration by weight. The spectra are labeled with the volume ratio of SWNT−COOH (0.01 mg/mL) to PABS (0.01 mg/mL). The dashed line is the spectrum of SWNT−PABS copolymer (0.01 mg/mL).

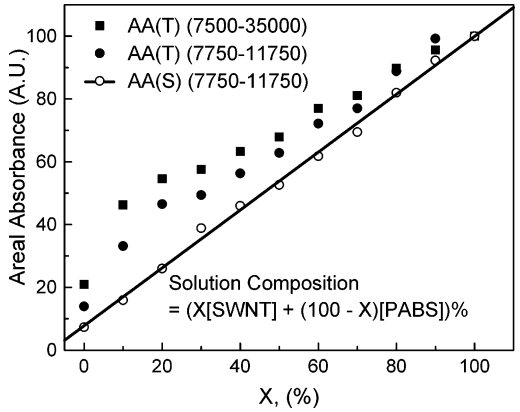

Figure 10. Plot of SWNT−COOH content in the mixture against the areal absorbance of the corresponding spectra (Figure 9). The solid square symbol is the areal integration with spectral cutoff from 7 500 to 35 000 cm^{-1}, the solid circular symbol is the areal integration with spectral cutoff from 7 750 to 11 750 cm^{-1}, and the hollow circular symbol is the areal integration above the baseline with spectral cutoff from 7 750 to 11 750 cm^{-1} and is mainly due to the S_{22} interband transition of the SWNTs.

This is best accomplished by taking the ratio of the effective extinction coefficients of SWNT−COOH and SWNT−PEG in the region of the S_{22} interband transition, to give a SWNT loading of 9.2/12.8 = 72% in SWNT−PEG, which is consistent with the TGA result.

Figure 8 shows the UV/Vis/NIR absorption spectra of PABS, SWNT−COOH, and SWNT−PABS in aqueous solution at a concentration of 0.02 mg/mL. The absorbance centered at 17750 cm^{-1} in the spectrum of PABS has been assigned to the n → π^* band transition,[39] whereas the SWNT−COOH spectrum shows the characteristic S_{22} interband transition centered at 9750 cm^{-1}. In the low-energy region, there is an obvious transfer of spectral weight from the region of the S_{22} SWNT interband region (∼10 000 cm^{-1}) to a part of the spectrum (∼16 500 cm^{-1}), which is near where the n → π^* transition of PABS occurs (17 750 cm^{-1}).[39] To understand the electronic properties of SWNT−PABS, we carried out a normalized least-squares fit of the spectra of neat SWNT−COOH and PABS to the spectrum of SWNT−PABS (Figure 8). The best fit to the experimental spectrum of SWNT−PABS was obtained with the function FIT = 0.22 × PABS + 0.78 × SWNT−COOH, and a difference spectrum was obtained from the relationship DIF = SWNT−PABS − FIT. The weighting factors resulting from the NIR fit are clearly at variance with our previous estimation of the SWNT loading of ∼30% in SWNT−PABS from TGA analysis (above). Taken together with the significant deviations exhibited by the difference spectrum, it is apparent that the SWNT−PABS spectrum is not a simple additive composite of the SWNT−COOH and PABS spectra, and this result provides clear evidence for an electronic interaction between the PABS and SWNT functionalities in sharp contrast with the behavior of SWNT−PEG discussed above.

To further understand the nature of the electronic interaction between SWNT and PABS, we separately prepared aqueous solutions of SWNT−COOH and PABS, each at a concentration of 0.01 mg/mL. These standard solutions were used to prepare a series of mixed solutions of different composition (Figure 9). It is clear that the SWNT−COOH component is the strongest absorber in this spectral region.

Figure 10 shows a plot of the areal absorbance between two spectral cutoffs (7 500−35 000 cm^{-1}, NIR−Vis−UV region and 7 750−11 750 cm^{-1}, S_{22} interband transition of SWNTs), as a function of the relative concentration of the two components (SWNT−COOH and PABS). While the intensity due to the nanotube S_{22} interband transition follows an approximately linear dependence on SWNT concentration, it is apparent that the spectral weight captured by the other areal absorbances initially grows very rapidly as the SWNT component is added, before following a more gradual increase. This confirms that there is

(57) Li, Y.-H.; Wang, S.; Luan, Z.; Ding, J.; Xu, C.; Wu, D. *Carbon* **2003**, *41*, 1057−1062.
(58) Zhao, L.; Gao, L. *Colloids Surf., A* **2003**, *224*, 127−134.
(59) Gao, B.; Yue, G. Z.; Qui, Q.; Cheng, Y.; Shimoda, H.; Fleming, L.; Zhou, O. *Adv. Mater.* **2001**, *23*, 1770−1773.
(60) Bahr, J. L.; Mickelson, E. T.; Bronikowski, M. J.; Smalley, R. E.; Tour, J. M. *Chem. Commun.* **2001**, 193−194.
(61) Zhou, B.; Lin, Y.; Li, H.; Huang, W.; Connell, J. W.; Allard, L. F.; Sun, Y. P. *J. Phys. Chem. B* **2003**, *107*, 13588−13592.
(62) Zhao, B.; Itkis, M. E.; Niyogi, S.; Hu, H.; Perea, D.; Haddon, R. C. *J. Nanosci. Nanotech.* **2004**, *4*, 995−1004.
(63) Zhao, B.; Itkis, M. E.; Niyogi, S.; Hu, H.; Zhang, J.; Haddon, R. C. *J. Phys. Chem. B* **2004**, *108*, 8136−8141.
(64) Sen, R.; Rickard, S. M.; Itkis, M. E.; Haddon, R. C. *Chem. Mater.* **2003**, *15*, 4273−4279.
(65) Hu, H.; Zhao, B.; Itkis, M. E.; Haddon, R. C. *J. Phys. Chem. B* **2003**, *107*, 13838−13842.

an electronic interaction between SWNT−COOH and PABS that at the very least is changing the nature of the chromophores in the mixture. On the basis of the sensitivity of the electrical conductivity of SWNT−PABS to environmental gases such as ammonia,[45] it seems likely that the electronic interaction may not be confined to the excited-state behavior and may involve a ground-state charge-transfer process. In this sense, SWNT−PABS represents the first SWNT graft copolymer in which the electronic structure should be regarded as a hybrid of the two components. This result also explains why the NIR spectrum of SWNT−PABS copolymer is not a simple sum of the two components and does not reflect the amounts of each component.

Conclusion

We report the synthesis of SWNT−PABS and SWNT−PEG graft copolymers from EA SWNTs at the gram scale. On the basis of mid-IR spectroscopy, we conclude that the PABS and PEG are covalently bonded to the SWNTs via amide and ester functionalities, respectively. The solubility of both copolymers is about 5 mg/mL in water. These SWNT graft copolymers have a fairly uniform length and diameter. On the basis of TGA measurements, we estimate the loading of SWNTs in SWNT−PABS and SWNT−PEG to be about 30 and 71%, respectively. The NIR spectrum of the SWNT−PABS graft copolymer is not a simple sum of the SWNT and PABS spectra, and we conclude that this is the first nanotube-based graft copolymer that has a ground state that is a hybrid of the electronic structures of the isolated macromolecular components. These graft copolymers are well suited for use in the preparation of composite materials,[66] in biological research,[46] and for the active element of electronic sensors.[45]

Acknowledgment. This research was supported by DOD/DARPA/DMEA under Award No. DMEA90-02-2-0216. Carbon Solutions, Inc., acknowledges a DARPA Phase I SBIR Award administered by the U.S. Army Aviation and Missile Command (Award No. W31P4Q-04-C-R171) and AFOSR Phase I STTR Award No. FA9550-04-C-0122.

JA042924I

(66) Sen, R.; Zhao, B.; Perea, D. E.; Itkis, M. E.; Hu, H.; Love, J.; Bekyarova, E.; Haddon, R. C. *Nano Lett.* **2004**, *4*, 459−464.